We really thank the reviewer for the positive and helpful comments. Now the manuscript has been revised accordingly. Our responses are written in blue text. A version of the revised manuscript was provided as a supplement.

Anonymous Referee #2

1. The paper investigates the abundance, speciation and spectral absorption of iron oxides in five glaciers in the Tibetan Plateau. Samples were collected on the field and analyzed in the laboratory to retrieve their composition in terms of iron oxides, black carbon and organic matter. Measurements of the spectral absorption were performed on the collected samples and the partitioning of the absorption due to mineral dust, black carbon, and organic material was estimated. The study is quite an interesting contribution and in my opinion it deserves publication in "The Cryosphere". I have nonetheless few comments concerning the data treatment and discussion that I will detail in the following. I have in particular some doubt on the choices performed to treat absorption measurements and I would like the authors to improve this part by adding more details and by performing some sensitivity calculations.

Reply: Thank you for the recognition of our work. We have added more details about the absorption measurements and performed sensitivity calculations in the manuscript. "Because the ISSW spectrophotometer is only sensitive to the signal of light absorption but not scattering of LAIs on filters due to its integrating sandwich structure, he light attenuation by samples on filter at specific wavelength will be converted to equivalent BC mass loading" (See Line 11-14, Page 5). "The standard deviation between repeated measurements range from 0.29% to 7.83% (mean value: 2.92%) in this study, which falling into the recommended variation range (i.e., < 10%) by Grenfell et al. (2011)." (See Line 23-24, Page 5).

2. Abstract: please define what Cryoconite is also in the abstract.

Reply: Changed. (See Line 17-18, Page 1)

3. Section 2.6: In the procedure for MAC estimate of cryoconite you need to make assumptions on the MAC and you assume the MAC of fullerene, i.e. a proxy for BC, in your calculations. First, I am not sure to completely understand the procedure followed to retrieve the MAC of cryoconite and I would ask the authors to provide more details on this part.

Reply: Thanks for this comment. The ISSW method we used is originally established by Grenfell et al. (2011) and subsequently employed to analyze the light absorbing impurities in snow from North American (Dang and Hegg, 2014), Northern China (Wang et al., 2013) and Arctic (Forsstrom et al., 2013). The ISSW spectrophotometer measures the light attenuation spectrum by LAIs on filters. Then, the light attenuation was calibrated against a set of standard BC samples (i.e., fullerene) to determine the equivalent BC loading, which could produce the same amount of light attenuation by LAIs on filter. Because the ISSW system is sensitive to light absorption but not scattering owning to the enhanced absorption signal result from its diffuse radiation field and integrating sandwich sphere (Grenfell et al., 2011), the absorption optical depth of LAIs could derived from the multiplication between equivalent BC loading and its MAC (0.63 m^2 g^{-1} at 550 nm). The MAC of cryoconite was then calculated from dividing the optical depth by the mass loading of LAIs.

Second, I wonder: which is the impact of the assumption on the MAC on the obtained results? I mean, what is the uncertainty in the retrieved MAC of cryoconite due to the fact of assuming the MAC of fullerene in calculations? It would have not been more appropriate to use a weighted average MAC between BC, dust, and organics based on their mass contribution to cryoconite estimated deposits? For a reference of the MAC of dust see for example the recent paper by Caponi et al. (2017).

Reply: According to the previous research, the relative uncertainty in MAC of fullerene is no more than 6.6% by the ISSW method (Zhou et al., 2017). And based on the study by Grenfell et al. (2011), the main uncertainties in this method derived from instrumental uncertainty and nonuniformities in the sample deposition on filter, which could be evaluated by repeated measurement. In our study, the standard deviation

between repeated measurement range from 0.29% to 7.83% (mean value: 2.92%) (See Line 23-24, Page 5), which falls into the recommended variation range (i.e., < 10%) by Grenfell et al. (2011). This demonstrate the high reliability of our method used to analyze the optical properties of cryoconite.

Regarding the second question, as our understanding on your suggestions, the weighted average MAC of cryoconite could be calculated by the following formula:

$$MAC_{cyroconite} = MAC_{dust} \cdot f_{dust} + MAC_{BC} \cdot f_{BC} + MAC_{OM} \cdot f_{OM}$$

However, the relative mass concentration of organic matters in cyroconite (f_{OM}) is unknown, although the BC and iron oxides were determined. More important, the light absorption properties of organics, such as AAE, could range from 2 to 11 at different environments (Laskin et al., 2015), due to their complicated sources and composition (HULIS or algae). Therefore, it will lead to high uncertainty in the weighted average MAC of cryoconite if we simply assume a MAC value for organic matters. Considering the two reasons above, we intend to obtain the MAC of cryoconite directly using the ISSW method.

4. Always concerning Sect. 2.6, if available, it would have not been useful also to calibrate light attenuation against pure hematite and goethite minerals? This point has been probably already raised by the other reviewer, but I repeat the question.

Reply: Thanks for this comment. Actually, using standard black carbon (i.e. fullerene) is well established for the ISSW measurement. In details, the calibration is based on a set of seven standard filters with a series of loadings of fullerene, a commercially produced soot. These were prepared through sequential dilutions and gravimetric confirmation of a standard soot suspension obtained after previous filtration through 2.0 μm and 0.8 μm pore Nuclepore filters (Grenfell et al., 2011). The filter loadings span a range sufficient to define the instrument sensitivity curves for field samples over the full visible spectral band of interest. In contrast, these reference filters by hematite or goethite is not available currently.

5. Sections 3.3 and 3.4: take into account the Caponi et al. (2017) reference values for the MAC in the calculations. Also, iron oxide and their speciation for dust samples from many regions worldwide were reported in that work, and these data can be useful for your data interpretation.

Reply: Thank you for this valuable comment. We have considered the results in the recommended paper during the discussion. (See Line 16-17, Line 31-32, Page 6; Line 4-6, Page 8).

6. Sections 3.3 and Conclusions: I guess one interesting point to discuss based on your results and the comparison with the literature is the regional scale variability of iron content and its speciation and the impact on glacier absorptivity and albedo. I would develop this aspect more in the discussion. Could you also add some calculations of how much spectral albedo would change in relation to absorption by different species as found in your study? What about the seasonal and spatial representativeness of your data?

Reply: Thanks. We agree with the reviewer that it will be better to calculate the radiative effect of LAIs in cryoconite. Unfortunately, it is beyond our ability to do this in this work. We are focusing on the chemical compositions and light absorption parameters (i.e., MAC and AAE) of LAIs in this study. Currently, due to the limitation of our field sampling, we can not obtain the spatial distribution of cryoconite on the glacier surface (i.e. the percentage of cryoconite cover in a unit of glacier surface area). In the future research, we will explore quadrat sampling to reveal the exact change of albedo by cryoconite. Now we have noted this point in the final section of this paper (Line 17-20, Page 9).

Cryoconite mainly formed in the ablation zone on glacier, which indicates they are more active during summer season. Therefore, we only collected the cryoconite samples during summer time, as listed in Table 1. Now we have added this point in the text (Line 21-23, Page 3). The five research sites represent different geographic environments cross the Tibetan Plateau from north to south, which have been specifically described in Section 2.1. Regarding the spatial representativeness (Line 3-

7, Page 9), the glacier (i.e. BS) located in the southeast margin of Tibetan Plateau presents distinct pattern of the iron speciation (shown in Fig 4) and apportion of different constituents to the light absorption. The most plausible reason is that glacier is strongly impacted by anthropogenic emissions nearby, with the highest contents of black carbon and organic matters in cryoconites.

7. Section 3.3, Page 7, line 8: do you mean the effect of atmospheric aging on minerals? Please be more specific.

Reply: It is similar to the atmospheric aging but take place on the surface of glacier. Just as mentioned in line 4 -5 on page 7, goethite is favored in moist and cool conditions while hematite commonly occurs in warm and dry environment. Therefore, hematite may tend to transfer into goethite on the moist and cool cryoconite surface. Microorganisms may also play a crucial role in the degradation of rocks and minerals in terrestrial environment through changing the transformation rates, pathways, and even the end products (Fru et al., 2012). But more research is needed to test the hypothesis (Line 22-25, Page 7).

8. Page 8, lines 8-11: I guess this is basically your key conclusion and I would move it to Sect. 4. Also I suggest to add a brief discussion on the impact of the regional variability of iron oxides and their speciation, and the representativeness of your results compared to other regions of the world under the influence of other deserts with different mineralogical compositions.

Reply: We have moved the sentence (see Line 12-14, Page 9). And the spatial representativeness of our results was discussed (Line 3-7, Page 9).

References:

Dang, C., Hegg, D.A., 2014. Quantifying light absorption by organic carbon in Western North American snow by serial chemical extractions. Journal of Geophysical Research-Atmospheres 119.

Forsstrom, S., et al., 2013. Elemental carbon measurements in European Arctic snow packs. Journal of Geophysical Research-Atmospheres 118, 13614-13627.

Fru, E.C., Piccinelli, P., Fortin, D., 2012. Insights into the Global Microbial Community Structure Associated with Iron Oxyhydroxide Minerals Deposited in the Aerobic Biogeosphere. Geomicrobiology Journal 29, 587-610.

Grenfell, T.C., Doherty, S.J., Clarke, A.D., Warren, S.G., 2011. Light absorption from particulate impurities in snow and ice determined by spectrophotometric analysis of filters. Applied Optics 50, 2037-2048.

Laskin, A., Laskin, J., Nizkorodov, S.A., 2015. Chemistry of Atmospheric Brown Carbon. Chemical Reviews 115, 4335-4382.

Wang, X., Doherty, S.J., Huang, J., 2013. Black carbon and other light-absorbing impurities in snow across Northern China. Journal of Geophysical Research-Atmospheres 118, 1471-1492.

Zhou, Y., et al., 2017. Quantifying Light Absorption of Iron Oxides and Carbonaceous Aerosol in Seasonal Snow across Northern China. Atmosphere 8.

Iron oxides in the cryoconite on the glaciers over Tibetan Plateau: abundance, speciation and implications

Zhiyuan Cong[1, 5, *], Shaopeng Gao[1], Wancang Zhao[3], Xin Wang[4], Guangming Wu[1, 6], Yulan Zhang[2], Shichang Kang[2, 5, *], Yongqin Liu[1], and Junfeng Ji[3]

[1]Key Laboratory of Tibetan Environment Changes and Land Surface Processes, Institute of Tibetan Plateau Research, Chinese Academy of Sciences, Beijing 100101, China
[2]State Key Laboratory of Cryospheric Sciences, Northwest Institute of Eco-Environment and Resources, Chinese Academy of Sciences, Lanzhou 730000, China
[3]Key Laboratory of Surficial Geochemistry, Ministry of Education, School of Earth Sciences and Engineering, Nanjing University, Nanjing 210023, China
[4]Key Laboratory for Semi-Arid Climate Change of the Ministry of Education, College of Atmospheric Sciences, Lanzhou University, Lanzhou 730000, China
[5]CAS Center for Excellence in Tibetan Plateau Earth Sciences, Beijing 100101, China
[6]University of Chinese Academy of Sciences, Beijing 100049, China

Correspondence to: Zhiyuan Cong (zhiyuancong@itpcas.ac.cn) or Shichang Kang (shichang.kang@lzb.ac.cn)

Abstract. Cryoconite is the mixture by incoherent impurities and ice with dark color presented in the ablation zone of glacier. As an important constituent of light-absorbing impurities on the glacier surface, iron oxides determine the radiative impact of mineral dust. In particular, the distinct optical properties between hematite and goethite highlight the necessity to obtain accurate knowledge about their abundance and speciation. Cryoconite samples from five glaciers in different region of Tibetan Plateau (TP) and surroundings were studied. The iron abundances in the cryoconite from TP glaciers ranged from 3.40% to 4.90% by mass, which reflected a natural background level. Iron oxides were extracted and determined using diffuse reflectance spectroscopy. The ratios of free to total iron for the five glaciers ranged from 0.31 to 0.70, emphasizing that iron in the form of oxides should be considered rather than total iron in the albedo and radiative modelling. Furthermore, the goethite content in iron oxides (in mass fraction) ranged from 81% to 98%, showing that goethite is the predominant form among the glaciers. Using the abundance and speciation of iron oxides as well as their optical properties, the total light absorption were quantitatively attributed to goethite, hematite, black carbon and organic matters at 450 nm and 600 nm wavelengths. We found that the goethite played a stronger role than BC at shorter wavelength for most glaciers. Such findings are essential to understand the relative significance of anthropogenic/natural effect, and then taking the proper mitigation measures.

1 Introduction

The light-absorbing impurities (LAIs) in glaciers could significantly reduce the surface albedo of snowpack and absorb more solar energy (Warren and Wiscombe, 1985). LAIs were recognized as a major contributor to the glacier and ice sheet melting (Qian et al., 2015), along with the rising air

temperatures (IPCC, 2014). The composition of LAIs on the glacier surface is very complex. Their major constituents include black carbon, brown carbon, soil dust, as well as biogenic matter (Baccolo et al., 2017; Kaspari et al., 2015; Pu et al., 2017; Takeuchi, 2002). The complex of LAIs is particularly the case for the mountain glaciers in Himalayas and Tibetan Plateau (TP) (Fig. 1). In summer, their surfaces are commonly covered by incoherent impurities (granular sediment) with dark color, which was termed as cryoconite (Baccolo et al., 2017; Dong et al., 2016).

Presently, tremendous attention has been paid to the black carbon (Kaspari et al., 2011; Wang et al., 2015; Yasunari et al., 2010), partly because the cryosphere region of TP is in the vicinity of intensive BC source region, e.g. South Asia, and is receiving strong influences from those anthropogenic emissions (Cong et al., 2015a). Nevertheless, few research focus on dust in this region despite the observation that dust is apparently the predominant constituent of impurities on the glacier surface, especially in its ablation area (Qian et al., 2015). Based on field research at Mera Glacier of Nepal Himalayas, Kaspari et al. (2014) pointed out that when dust loading is high, the snow albedo reduction and subsequent radiative forcing caused by dust will overwhelm black carbon.

To quantify the relative contribution of dust and black carbon as well as other substances is challenging (Painter et al., 2010). In the snow albedo simulation model like SNICAR (Flanner and Zender, 2006), dust concentration (micrograms of dust per gram of ice) was employed to represent the loading of dust, without considering the dust composition. Actually, the light-absorption capacity of dust essentially depends on the presence of iron oxides (also commonly termed as “free iron”) (Alfaro et al., 2004; Moosmüller et al., 2012; Shi et al., 2012). The most common iron oxide species in nature are hematite (Fe_2O_3) and goethite (FeO(OH)), which have distinct optical properties in terms of absorption and wavelength dependence (Balsam et al., 2014). At the same time, some parts of iron are incorporated into the crystal lattice of alumino-silicates (defined as structural iron), and they do not contribute to the absorption of solar light (Lafon et al., 2006).

Up to now, the iron abundance and especially its mineral phases in glacial area are not well understood (Shahgedanova et al., 2013). The degree to which iron oxides contribute to solar absorption and reduction of snow albedo remain uncertain. To constrain the uncertainties of estimating the radiative forcing of cryoconite, particularly in the Tibetan Plateau glacier area, we designed this research to address several key issues. Firstly, what is the abundance of iron in the cryoconite of mountain glaciers? How much fraction of the total iron exists as iron oxides with efficient light-absorption capability? What is the relatively proportion of hematite and goethite, considering their distinct optical characteristics? What is their spatial variation in different types of glacier? Furthermore, how do the iron oxides impact the absorbing properties of cryoconite?

2 Field sampling and laboratory measurements

2.1 Field sampling

In order to examine geographic variability, five glaciers in different region of TP and surroundings were chosen for the cryoconite sampling (Fig. 2). The detailed descriptions on the location and

elevation are summarized in Table 1. Urumqi No. 1 Glacier (43°06′N, 86°49′E) (hereafter donated as UG), with two branches covering 1.646 km^2, is located in eastern Tien Shan. The air circulation regime there is dominated by the westerlies in summer and the Siberian High in winter (Wang et al., 2014). Laohugou Glacier (donated as LHG), with a length of 10 km and an area of 20 km^2, is at the northern slope of western Qilian Mountains with typical continental climatic conditions (Dong et al., 2014). That area is surrounded by large sandy deserts in Northwest China, like Taklimakan Desert to the west, Qaidam Basin to the southwest and the Gobi Desert to the north. Xiaodongkemadi Glacier (donated as XDK) is located on the northern slope of Tanggula Mountains, center of Tibetan Plateau. Previous studies showed that Tanggula Mountain is the north most boundary of the South Asian monsoon influence. Palong #4 Glacier (donated as PL), located in the southeast Tibetan Plateau, is a typical temperate glacier. It is strongly influenced by the South Asian summer monsoon intruding via the Brahmaputra Valley, and characterized by high accumulation (2500-3000 mm) and ablation rates on an annual scale (Yang et al., 2015). Baishui No. 1 Glacier (donated as BS), with length 2.26 km and area 1.32 km^2, is the largest glacier in Yulong Mountains, southeast margin of Tibetan Plateau. It is characterized by high precipitation, low snow line, and relatively high temperatures (equilibrium line mean annual value -6 °C, summer value 1-5 °C) (Niu et al., 2013).

Cryoconite samples were collected using a stainless-steel scoop on the surfaces of five glaciers described above. Samples were preserved in NALGENE HDPE wide-mouth bottles (500 ml) and kept in frozen until analysis. In the laboratory the cryoconite samples were freeze-dried, turning into powder for the subsequent determination. Therefore, in this work, the cryoconite refers to the dried mass of cryoconite, excluding the water (snow or ice) contents. Cryoconite mainly formed in the ablation zone on glaciers in summer season. Therefore, as the sampling protocol, our research mainly reflects the scenario happened in summer on the glacier surface.

2.2 Elemental analysis by ICP-MS

A portion of cryoconite sample was digested in a laboratory hood into 1% HNO_3 (Optima Grade, Fisher Co.), then measured by inductively coupled plasma-mass spectrometry (ICP-MS, Thermo X7, Thermo-Elemental Corp.) for Fe and other elements. The accuracy and precision of trace elements was ascertained based on repeated measurement of the USGS Geochemical Reference Standard (Andesite, AGV-2). The measured and certified values for Fe agree well, with recovery better than 95%. The detailed description of the analytical protocol could be found in previous work (Cong et al., 2015b; Wu et al., 2009).

2.3 Total organic carbon and black carbon

The contents of organic carbon were determined by a total carbon analyzer (TOC-V, Shimadzu). The accuracy of the TOC analysis was ±5%. The separation and analysis of black carbon in the cryoconite were adopted from the procedures previously developed for sediments (Cong et al., 2013; Han et al., 2011). Specifically, the samples were first freeze-dried, grinded into powder and weighed. Then, HCl (2N) was added, to remove carbonates, silicates, and some kinds of metal oxides. The solution was

centrifuged to remove the supernatants. Then mixture (1:2) of HCl (6N) and HF (48%) were added into the residue and reacted further. Finally, the residual solid was diluted with ultrapure water, filtered by quartz fiber filter with even distribution on their surface (QMA grade; Whatman International Ltd, England). The quartz filters were analyzed for BC using a DRI model 2001 carbon analyzer. For quality control, standard reference material (marine sediment, NIST SRM-1941b) was also analyzed (Cong et al., 2013).

2.4 Extraction and quantification of iron oxides

Cryoconite samples were treated with Citrate-Bicarbonate-Dithionite (CBD) method three times to completely extract iron oxides (Ji et al., 2002; Lafon et al., 2004; Mehra and Jackson, 1958). Then dissolved Fe^{3+} concentrations in the CBD solution were determined by a UV-2100 spectrophotometer (UNICO Inc., Shanghai) to obtain the iron mass in the form of oxides, Fe(ox), relevant to the light-absorption in the visible light. The remaining iron, i.e. the structural iron, was calculated by subtracting the Fe(ox) from total iron.

$$Fe(struc) = Fe(tot) - Fe(ox)$$

Here, Fe(tot) is the total iron concentration achieved from ICP-MS elemental analysis.

2.5 Hematite/goethite measurement using Diffuse Reflectance Spectroscopy

Given the low abundance of Fe in the cryoconite, the speciation of iron oxides can not be achieved by traditional mineralogical analysis methods like X-ray diffraction (XRD). In this study, diffuse reflectance spectroscopy (DRS) was employed to distinguish and quantify hematite and goethite. Measurements were conducted using a Perkin-Elmer lambda 900 spectrophotometer (Perkin-Elmer Corp., Norwalk, CT) equipped with a diffuse reflectance attachment. Analyses were performed for spectra in the range from 400 to 700 nm with an interval of 2 nm. Detailed procedures have been well described previously (Ji et al., 2002; Lu et al., 2017).

A set of calibration samples containing known hematite were measured. Then the percent reflectance in red color band (630-700 nm, redness) was used as an independent variable in a transfer function for calculating hematite, which was established through regression as following:

$$Hm(wt.\ \%) = 1E\text{-}06 \cdot e^{27.37 * Redness} \quad (R^2_{adj} = 0.9301,\ RMSE = 0.3018)$$

Assuming the CBD-extracted Fe (in the form of iron oxides) are only constituted by hematite (Hm) and goethite (Gt), the content of goethite could be calculated using the following equation:

$$Gt\ (wt.\ \%) = 1.59 \times (Fe_{(ox)}\text{-}Hm/1.43)$$

The reproducibility standard deviation of reflectance at all wavelengths was less than 0.15% (Lu et al., 2017).

2.6 Light absorption of cryoconite

Measurements of light absorption were performed using an ISSW spectrophotometer in Lanzhou University, China. The experimental strategy was mainly based on the method described by Doherty et al. (2010) and Wang et al. (2013). The ISSW measurement system are specially designed to be sensitive to light absorption and to avoid the interference of light scattering (Grenfell et al., 2011). The ISSW spectrophotometer could provide the spectral absorption properties of cryoconite, by weighting the transmitted light (I) for a sample and that for a blank filter (I_0). The relative attenuation (x_λ) described by the natural logarithm of I_0 / I:

$$x_\lambda = \ln[I_0(\lambda)/I(\lambda)] \quad (1)$$

The spectrum of light attenuation was further calibrated by a set of black carbon standards (fullerene soot, Alfa Aesar, Inc., Ward Hill, MA, USA) (Fig. S1). Because the ISSW spectrophotometer is only sensitive to the signal of light absorption but not scattering of LAIs on filters due to its integrating sandwich structure, the light attenuation by samples on filter at specific wavelength will be converted to equivalent BC mass loading (L_{BC}, μg C cm^{-2}), which allows to calculate absorption optical depth $\tau(\lambda)$ by cryoconite: $\tau_\lambda = L_{BC}\beta_\lambda$. Where β_λ is mass absorption coefficiency (MAC) of standard black carbon (i.e., fullerene, 6.3 m^2 g^{-1} at 550 nm) (Grenfell et al., 2011; Zhou et al., 2017). Then the light absorption capacity of cryoconite was calculated through dividing the absorption optical depth by the mass loading on filter:

$$\mathrm{MAC} = \tau_\lambda / \mathrm{L} \quad (2)$$

The absorption Ångström exponent (AAE) describes the wavelength dependence of the light absorption by particles (Ångström, 1929). The value of AAE could obtained by the formula of: $\mathrm{AAE} = -\ln(\tau_1/\tau_2)/\ln(\lambda_1/\lambda_2)$, where τ_1 and τ_2 are the light attenuation calculated at given wavelength λ_1 and λ_2, respectively. The standard deviation between repeated measurement range from 0.29% to 7.83% (mean value: 2.92%).

3 Results and discussion

3.1 Organic carbon and black carbon contents

The total organic carbon and black carbon mass fractions of the cryoconite from the five glaciers are presented in Figure 3. The most striking feature was that BS exhibited the highest TOC content (9.70 ± 0.99 % in mass faction), about 4 times higher than other four glaciers. Similarly, the BC in the cryoconite from BS were also significantly higher than other glaciers, i.e. UG, LHG, XDK and PL. For the black carbon concentration, BS glacier also has the highest abundance (1.99 ± 0.28% in mass), indicating the strong anthropogenic (fossil fuel and biomass burning) influence there. For the remaining four glaciers, their black carbon contents were comparable, ranging from 0.06 ± 0.01% (in total mass of dried cryoconite) of XDK to 0.13 ± 0.03% of PL. For comparison, Di Mauro et al. (2017)

reported the black carbon values in cryoconites from Morteratsch Glacier (Swiss Alps), with the range of 0.30 - 0.4 % in mass faction.

3.2 Abundance of elemental Fe (total) and free-Fe (iron oxides)

The iron contents found in cryoconite samples from UG, LHG, XDK, PL and BS glaciers averaged 4.62%, 4.28%, 3.40%, 4.18% and 4.90%, by mass, respectively (Figure 4). Our data were similar to the previous reported iron contents in dust particles preserved in ice cores across Tibetan Plateau (Wu et al., 2012), which ranged from 3.38% to 5.41%. The iron in the cryoconite on the TP glaciers represents a natural background level. Lower iron contents were found in the dust layers deposited on snow cover in northern Utah, USA (the Wasatch Range), which varied from 1.73 to 2.85% by mass (Reynolds et al., 2014). Given the scarce information of Fe abundance available in the glacier area, we also briefly summarized the data in mineral dust from various desert regions worldwide for comparison (Table 2). The determined Fe contents in desert aerosols from ZBT (ZhengBeiTai) and Yulin in North China were 5.38% and 7.7% in total dust aerosol mass, respectively, somewhat higher than our values of cryoconite over glaciers. The reported values of Fe content from Sahara and Arabian Peninsula generally varied in the range from 2.0 to 11% by mass (Gao et al., 2001; Gomes and Gillette, 1993; Zhang et al., 2015), depending on the locations and the transport process. Recently, Caponi et al. (2017) reported the mass fraction of Fe in global dust aerosols ($PM_{10.6}$) ranged from 2.8% (Namibia) to 7.3 (Australia). In addition, in this study there was no systematic variation of the Fe concentrations with altitude, which indicated that the cryoconite on each glacier was homogeneous mixture. The comparable levels of iron (3.4% -4.9%) found in the five glaciers in different parts of TP demonstrated that there is little regional variability of elemental iron in the cryoconites, which is likely related to the mineralogical composition of parent soils.

Because only iron oxides (free iron) could effectively control the absorbing property of mineral materials, the content of free iron is more concerned in radiative and climate modelling. Table 2 shows the means of free and structural iron in cryoconite (percentage in total mass) from the five glaciers, with their standard deviations. Interesting, the highest value of total Fe and the highest free-to-total ratio were found in the samples from BS. The color of BS samples was darker than others visually, and they also present the highest TOC contents among the five glaciers (Fig. 3).

The ratios of free to total iron for the five glaciers ranged from 0.31 to 0.70 (Table 2). That means substantial Fe are trapped in the crystal lattice (i.e. structural Fe) and has no direct relationship with the light absorption. This finding is generally in agreement with that of Lafon et al. (2004) and Caponi et al. (2017) for desert aerosols (Table 2). Namely, only about half total-iron is under the form of iron oxides. Therefore, our result clearly demonstrates that the total iron is not suitable to be directly used in the albedo and radiative modelling, although this has been a common practice in previous research (Kaspari et al., 2014; Wang et al., 2013). If this point was considered, the contribution of iron-containing minerals to the total light absorption on the glacier surface will decrease almost 50%, namely, the other light-absorbing components like black carbon and brown carbon should account for much larger fraction correspondingly.

3.3 The speciation of iron oxides

In previous modelling studies of the dust radiative forcing, hematite was usually assumed to be the major absorbing iron oxides (Sokolik and Toon, 1999). However, in this study goethite was found more abundant than hematite for all the five glaciers (Fig. 4 and Table 2). The goethite in total iron oxide mass ranged from 81% (for XDK) to 98% (for BS), showing that goethite is the predominant form of iron oxides. The ratios of goethite to hematite in our study were even higher than those reported for desert aerosols (Table 2) (Formenti et al., 2014; Lafon et al., 2006; Shen et al., 2006). For example, Lafon et al (2004) reported the iron oxides in the dust from Northwest China with about half of total iron in the form of iron oxides, and the abundance of goethite (73% of the total iron oxide mass) was higher than hematite (27%). Shen et al. (2006) determined comparable goethite/hematite composition data in dust aerosols from North China. i.e. 64% for goethite in total iron oxide mass and 36% for hematite in Dunhuang, 63% and 37% in Yulin, and 68% and 32% in Tongliao, respectively. While in the dust samples collected on the snow from American West (Wasatch Range, Utah), the amounts of goethite and hematite in dust samples were found roughly equal using Mössbauer spectroscopy (Reynolds et al., 2014).

Beside the pedogenic characteristics, the dominance of goethite over hematite may be also ascribed to the glacier surface environment. Goethite formation is favored in moist and cool conditions, while hematite commonly occurs in warm and dry environment (Reynolds et al., 2014). That is also why the ratios of goethite to hematite were frequently used as indicators of paleoclimate (e.g. precipitation and temperature) (Schwertmann, 1971). Taking into account the cold and humid conditions on the glacier surface, mineralogical transformation of hematite to goethite is highly expected to happen, resulting more goethite. Microorganisms may also play a crucial role in the degradation of rocks and minerals in terrestrial environment through changing the transformation rates, pathways, and even the end products (Fru et al., 2012). This is especially plausible for BS glacier with the highest TOC contents (an indicator of microbe) as well as iron oxides, but more research is needed to test the hypothesis.

3.4 Contribution to light absorption by cryoconite components

Optical properties of goethite and hematite, including MAC and AAE parameters, are critical to assess their role in the light absorption. A wide range of MAC values have been reported in the literatures. According to the previous work by Alfaro (2004), the mass absorption coefficient of iron oxides (goethite : hematite, 73% : 27%) in dust from Northwest China desert was measured as 0.56 m^2 g^{-1} at 660 nm, and it will increase about 6 times at shorter wavelength (325 nm) (AAE ≈ 3). This value was further employed to evaluate the albedo and radiative forcing effect of dust in snow of Himalayas (Nepal) (Kaspari et al., 2014). Recently, Utry et al. (2015) reported the MAC value of hematite (purity > 95%) as 0.54 m^2 g^{-1} at 532 nm, based on the measurements of a multi-wavelength photoacoustic instrument. Wang et al. (2013) choose the MAC of goethite of 0.9 m^2 g^{-1} (550 nm) and AAE value of 3 to assess the contribution of mineral dust to the total absorption of LAIs in North China snow. Based on the laboratory experiments by ISSW, we determined Fe-specific absorption coefficient using the

goethite (Stream Chemicals, Inc.) and hematite standard (Sigma Aldrich, Inc.) (Fig. 5). The calculated MAC values at 450 nm for goethite and hematite were 1.55 ± 0.08 m^2 g^{-1} and 1.12 ± 0.11 m^2 g^{-1}, respectively. And the MAC values at 600 nm were 0.15 ± 0.01 m^2 g^{-1} and 0.55 ± 0.03 m^2 g^{-1}, respectively. It should be noted that the MACs reported here are the values of isolated iron oxides (i.e., hematite and goethite). They are much larger than the MAC values of dust, which range from 0.013 m^2 g^{-1} to 0.055 m^2 g^{-1} over the world (Caponi et al., 2017).

Here we assumed that the total light absorption was entirely and exclusively caused by three components, i.e. iron oxides (goethite and hematite), BC and organic matters. Compared to dust and black carbon, the composition and sources of organic matters over the glacier surface are complicated. Organic matter was a mixture of soil humic and humic-like matters, biogenic particles (e.g., algae, fungi and plant debris) and biomass/fossil fuel burning emissions (Wu et al., 2018; Wu et al., 2016), which are often termed as brown carbon (BrC). Considering its diverse sources and complex composition, in this work we did not assume the specific optical parameters for organic matters. Instead, the relative contributions to absorption by organic matters were obtained by subtracting the portions by iron oxides and black carbon from the total absorption. The optical properties of the latter two components are much certain than light absorbing organics. The mass absorption efficiency and AAE value of BC were assumed to be 6.3 m^2 g^{-1} (550 nm) and 1.1, respectively (Grenfell et al., 2011).

Because the light absorption capability of iron oxides and organic matters vary with wavelength, here we calculated the relative absorption of these three components at 450 nm and 600 nm, respectively. As shown in Figure 6, at 600 nm (the right panel), the organic matters dominated the light absorption. And BC was the second contributor to the light absorption, especially for the BS glacier with the highest BC concentration. However, the contribution of iron oxides increases dramatically at 450 nm, especially for goethite, due to their high light absorption ability at short wavelength. For the glaciers except BS, the absorption by goethite was larger than BC and approximately equal to organic matters. The increased contribution by goethite at the shorter wavelength was due to its large AAE value (Zhou et al., 2017), which indicated stronger light absorption at short wavelength. While the relative contribution to absorption by hematite appeared to be constant between different wavelengths.

4. Summary and Conclusions

The degree to which mineral dust, especially iron oxides, affect the solar absorption and decreases of snow albedo remain uncertain. Despite their importance, the content and speciation of iron oxides in the cryoconite over the glacial surface has not been reported previously.

The iron abundances in the cryoconite from TP glaciers ranged from 3.40% to 4.90% by mass, which were comparable to the upper continental crust (UCC) composition (3.5% of Fe) (Taylor and McLennan, 1995) and implied their natural sources. We further separated and determined iron oxides (free Fe) using the Citrate-Bicarbonate-Dithionite method. The ratios of free to total iron for the five glaciers ranged from 0.31 to 0.70. That means substantial amounts of Fe are trapped in the crystal lattice (i.e. structural Fe) and has no direct influence on the light absorption. Our result clearly demonstrated that the total iron was not suitable to be directly used in the albedo and radiative modelling, although this is a common practice in previous studies. The iron oxides were further

quantified into goethite and hematite, the two major species. The goethite content in iron oxides (in mass fraction) ranged from 81% (XDK) to 98% (BS), showing that goethite is the predominant form of iron oxides. For the spatial representativeness, four glaciers (i.e. UG, LHG, XDK and PL) in the main body of TP demonstrated similar pattern regarding the iron oxide abundance and speciation. However, Baihui glacier is unique in these aspects. Baishui glacier is located at the southeastern margin of TP and closely adjacent to the intensive human activities area, and receives more organic matters. The microbe in such environment may perturb the nature distribution of iron.

Taking account of both the abundance of iron oxides and their optical properties, the total light absorption were quantitatively attributed to goethite, hematite, BC and organic matters at 450 nm and 600 nm. Organic matters were found to be the most important light absorber at 450 nm and 650 nm wavelengths. We demonstrated that the goethite played a stronger role than BC at shorter wavelength (i.e. 450 nm) for glaciers except Baishui (BS) glacier. Although iron oxides are much less absorbing than black carbon per unit mass, the much high mass concentration of mineral dust in the natural environment may result in total absorption be larger than BC. In general, this research provided new observations of the iron-oxides in glaciers, and the results are meaningful for understanding their role on mountain glacier surfaces in Himalayas and Tibetan Plateau, a climate sensitive and environmentally fragile region. Currently, due to the limitation of our field sampling, we can not obtain the spatial distribution of cryoconite on the glacier surface (i.e. the percentage of cryoconite cover in a unit area of glacier surface). In the future research, we will explore quadrat sampling to reveal the exact change of albedo by cryoconite.

Acknowledgements

We deeply thank Wei YANG, Yajun LIU, Hewen NIU, Junming GUO, Zhiwen DONG, Xiaofei LI, Yang LI and other team members for their contribution in the field sampling. This work is supported by National Science Foundation of China under Grants 41522103, 41522505, 41225002 and 41673095. The data used are listed in the references, tables, and supplements.

References

Alfaro, S. C., Lafon, S., Rajot, J. L., Formenti, P., Gaudichet, A., and Maille, M.: Iron oxides and light absorption by pure desert dust: An experimental study, Journal of Geophysical Research-Atmospheres, 109, 2004.

Ångström, A.: On the atmospheric transmission of sun radiation and on dust in the air, Geografiska Annaler, 11, 156-166, 1929.

Baccolo, G., Di Mauro, B., Massabò, D., Clemenza, M., Nastasi, M., Delmonte, B., Prata, M., Prati, P., Previtali, E., and Maggi, V.: Cryoconite as a temporary sink for anthropogenic species stored in glaciers, Scientific Reports, 7, 9623, 2017.

Balsam, W., Ji, J., Renock, D., Deaton, B. C., and Williams, E.: Determining hematite content from NUV/Vis/NIR spectra: Limits of detection, American Mineralogist, 99, 2280-2291, 2014.

Caponi, L., Formenti, P., Massabó, D., Di Biagio, C., Cazaunau, M., Pangui, E., Chevaillier, S., Landrot, G., Andreae, M. O., Kandler, K., Piketh, S., Saeed, T., Seibert, D., Williams, E., Balkanski, Y., Prati, P., and Doussin, J. F.: Spectral- and size-resolved mass absorption efficiency of mineral dust aerosols in the shortwave spectrum: a simulation chamber study, Atmos. Chem. Phys., 17, 7175-7191, 2017.

Cong, Z., Kang, S., Gao, S., Zhang, Y., Li, Q., and Kawamura, K.: Historical trends of atmospheric black carbon on Tibetan Plateau as reconstructed from a 150-year lake sediment record, Environmental Science & Technology, 47, 2579-2586, 2013.

Cong, Z., Kang, S., Kawamura, K., Liu, B., Wan, X., Wang, Z., Gao, S., and Fu, P.: Carbonaceous aerosols on the south edge of the Tibetan Plateau: concentrations, seasonality and sources, Atmospheric Chemistry and Physics, 15, 1573-1584, 2015a.

Cong, Z., Kang, S., Zhang, Y., Gao, S., Wang, Z., Liu, B., and Wan, X.: New insights into trace element wet deposition in the Himalayas: amounts, seasonal patterns, and implications, Environmental Science and Pollution Research, 22, 2735-2744, 2015b.

Di Mauro, B., Baccolo, G., Garzonio, R., Giardino, C., Massabò, D., Piazzalunga, A., Rossini, M., and Colombo, R.: Impact of impurities and cryoconite on the optical properties of the Morteratsch Glacier (Swiss Alps), The Cryosphere, 11, 2393-2409, 2017.

Doherty, S. J., Warren, S. G., Grenfell, T. C., Clarke, A. D., and Brandt, R. E.: Light-absorbing impurities in Arctic snow, Atmospheric Chemistry and Physics, 10, 11647-11680, 2010.

Dong, Z., Kang, S., Qin, D., Li, Y., Wang, X., Ren, J., Li, X., Yang, J., and Qin, X.: Provenance of cryoconite deposited on the glaciers of the Tibetan Plateau: New insights from Nd-Sr isotopic composition and size distribution, Journal of Geophysical Research: Atmospheres, 121, 7371-7382, 2016.

Dong, Z., Qin, D., Chen, J., Qin, X., Ren, J., Cui, X., Du, Z., and Kang, S.: Physicochemical impacts of dust particles on alpine glacier meltwater at the Laohugou Glacier basin in western Qilian Mountains, China, Science of The Total Environment, 493, 930-942, 2014.

Flanner, M. G. and Zender, C. S.: Linking snowpack microphysics and albedo evolution, Journal of Geophysical Research-Atmospheres, 111, 2006.

Formenti, P., Caquineau, S., Chevaillier, S., Klaver, A., Desboeufs, K., Rajot, J.-L., Belin, S., and Briois, V.: Dominance of goethite over hematite in iron oxides of mineral dust from Western Africa: Quantitative partitioning by X-ray absorption spectroscopy, Journal of Geophysical Research: Atmospheres, 119, DOI: 10.1002/2014JD021668, 2014.

Fru, E. C., Piccinelli, P., and Fortin, D.: Insights into the Global Microbial Community Structure Associated with Iron Oxyhydroxide Minerals Deposited in the Aerobic Biogeosphere, Geomicrobiology Journal, 29, 587-610, 2012.

Gao, Y., Kaufman, Y., Tanre, D., Kolber, D., and Falkowski, P.: Seasonal distributions of aeolian iron fluxes to the global ocean, Geophysical Research Letters, 28, 29-32, 2001.

Gomes, L. and Gillette, D. A.: A comparison of characteristics of aerosol from dust storms in central Asia with soil-derived dust from other regions, Atmospheric Environment. Part A. General Topics, 27, 2539-2544, 1993.

Grenfell, T. C., Doherty, S. J., Clarke, A. D., and Warren, S. G.: Light absorption from particulate impurities in snow and ice determined by spectrophotometric analysis of filters, Applied Optics, 50, 2037-2048, 2011.

Han, Y. M., Cao, J. J., Yan, B. Z., Kenna, T. C., Jin, Z. D., Cheng, Y., Chow, J. C., and An, Z. S.: Comparison of Elemental Carbon in Lake Sediments Measured by Three Different Methods and 150-Year Pollution History in Eastern China, Environmental science & technology, 45, 5287-5293, 2011.

IPCC: Climate change 2013: the physical science basis: Working Group I contribution to the Fifth assessment report of the Intergovernmental Panel on Climate Change, Cambridge University Press, 2014.

Ji, J. F., Balsam, W., Chen, J., and Liu, L. W.: Rapid and quantitative measurement of hematite and goethite in the Chinese loess-paleosol sequence by diffuse reflectance spectroscopy, Clays and Clay Minerals, 50, 208-216, 2002.

Kaspari, S., Painter, T. H., Gysel, M., Skiles, S. M., and Schwikowski, M.: Seasonal and elevational variations of black carbon and dust in snow and ice in the Solu-Khumbu, Nepal and estimated radiative forcings, Atmospheric Chemistry and Physics, 14, 8089-8103, 2014.

Kaspari, S., Skiles, S. M., Delaney, I., Dixon, D., and Painter, T. H.: Accelerated glacier melt on Snow Dome, Mount Olympus, Washington, USA, due to deposition of black carbon and mineral dust from wildfire, Journal of Geophysical Research-Atmospheres, 120, 2793-2807, 2015.

Kaspari, S. D., Schwikowski, M., Gysel, M., Flanner, M. G., Kang, S., Hou, S., and Mayewski, P. A.: Recent increase in black carbon concentrations from a Mt. Everest ice core spanning 1860-2000 AD, Geophysical Research Letters, 38, 2011.

Lafon, S., Rajot, J. L., Alfaro, S. C., and Gaudichet, A.: Quantification of iron oxides in desert aerosol, Atmospheric Environment, 38, 1211-1218, 2004.

Lafon, S., Sokolik, I. N., Rajot, J. L., Caquineau, S., and Gaudichet, A.: Characterization of iron oxides in mineral dust aerosols: Implications for light absorption, Journal of Geophysical Research-Atmospheres, 111, 2006.

Lu, W., Zhao, W., Balsam, W., Lu, H., Liu, P., Lu, Z., and Ji, J.: Iron Mineralogy and Speciation in Clay-Sized Fractions of Chinese Desert Sediments, Journal of Geophysical Research: Atmospheres, 2017. 2017.

Mehra, O. and Jackson, M.: Iron oxide removal from soils and clays by a dithionite–citrate system buffered with sodium bicarbonate, 1958, 317-327.

Moosmüller, H., Engelbrecht, J. P., Skiba, M., Frey, G., Chakrabarty, R. K., and Arnott, W. P.: Single scattering albedo of fine mineral dust aerosols controlled by iron concentration, Journal of Geophysical Research: Atmospheres 117, doi:10.1029/2011JD016909, 2012.

Niu, H., He, Y., Zhu, G., Xin, H., Du, J., Pu, T., Lu, X., and Zhao, G.: Environmental implications of the snow chemistry from Mt. Yulong, southeastern Tibetan Plateau, Quaternary International, 313–314, 168-178, 2013.

Painter, T. H., Deems, J. S., Belnap, J., Hamlet, A. F., Landry, C. C., and Udall, B.: Response of Colorado River runoff to dust radiative forcing in snow, Proceedings of the National Academy of Sciences of the United States of America, 107, 17125-17130, 2010.

Pu, W., Wang, X., Wei, H., Zhou, Y., Shi, J., Hu, Z., Jin, H., and Chen, Q.: Properties of black carbon and other insoluble light-absorbing particles in seasonal snow of northwestern China, The Cryosphere, 11, 1213-1233, 2017.

Qian, Y., Yasunari, T. J., Doherty, S. J., Flanner, M. G., Lau, W. K. M., Ming, J., Wang, H., Wang, M., Warren, S. G., and Zhang, R.: Light-absorbing Particles in Snow and Ice: Measurement and Modeling of Climatic and Hydrological impact, Advances in Atmospheric Sciences, 32, 64-91, 2015.

Reynolds, R. L., Goldstein, H. L., Moskowitz, B. M., Bryant, A. C., Skiles, S. M., Kokaly, R. F., Flagg, C. B., Yauk, K., Berquo, T., Breit, G., Ketterer, M., Fernandez, D., Miller, M. E., and Painter, T. H.: Composition of dust deposited to snow cover in the Wasatch Range (Utah, USA): Controls on radiative properties of snow cover and comparison to some dust-source sediments, Aeolian Research, 15, 73-90, 2014.

Schlitzer, R., 2017.

Schwertmann, U.: Transformation of Hematite to Goethite in Soils, Nature, 232, 624-625, 1971.

Shahgedanova, M., Kutuzov, S., White, K. H., and Nosenko, G.: Using the significant dust deposition event on the glaciers of Mt. Elbrus, Caucasus Mountains, Russia on 5 May 2009 to develop a method for dating and "provenancing" of desert dust events recorded in snow pack, Atmos. Chem. Phys., 13, 1797-1808, 2013.

Shen, Z. X., Cao, J. J., Zhang, X. Y., Arimoto, R., Ji, J. F., Balsam, W. L., Wang, Y. Q., Zhang, R. J., and Li, X. X.: Spectroscopic analysis of iron-oxide minerals in aerosol particles from northern China, Science of The Total Environment, 367, 899-907, 2006.

Shi, Z., Krom, M. D., Jickells, T. D., Bonneville, S., Carslaw, K. S., Mihalopoulos, N., Baker, A. R., and Benning, L. G.: Impacts on iron solubility in the mineral dust by processes in the source region and the atmosphere: A review, Aeolian Research, 5, 21-42, 2012.

Sokolik, I. N. and Toon, O. B.: Incorporation of mineralogical composition into models of the radiative properties of mineral aerosol from UV to IR wavelengths, Journal of Geophysical Research: Atmospheres, 104, 9423-9444, 1999.

Takeuchi, N.: Optical characteristics of cryoconite (surface dust) on glaciers: the relationship between light absorbency and the property of organic matter contained in the cryoconite. In: Annals of Glaciology, Vol 34, 2002, Winther, J. G. and Solberg, R. (Eds.), Annals of Glaciology, 2002.

Taylor, S. R. and McLennan, S. M.: The geochemical evolution of the continental crust, Reviews of Geophysics, 33, 241-265, 1995.

Utry, N., Ajtai, T., Pinter, M., Tombacz, E., Illes, E., Bozoki, Z., and Szabo, G.: Mass-specific optical absorption coefficients and imaginary part of the complex refractive indices of mineral dust components measured by a multi-wavelength photoacoustic spectrometer, Atmospheric Measurement Techniques, 8, 401-410, 2015.

Wang, M., Xu, B., Kaspari, S. D., Gleixner, G., Schwab, V. F., Zhao, H., Wang, H., and Yao, P.: Century-long record of black carbon in an ice core from the Eastern Pamirs: Estimated contributions from biomass burning, Atmospheric Environment, 115, 79-88, 2015.

Wang, P., Li, Z., Li, H., Wang, W., and Yao, H.: Comparison of glaciological and geodetic mass balance at Urumqi Glacier No. 1, Tian Shan, Central Asia, Global and Planetary Change, 114, 14-22, 2014.

Wang, X., Doherty, S. J., and Huang, J.: Black carbon and other light-absorbing impurities in snow across Northern China, Journal of Geophysical Research-Atmospheres, 118, 1471-1492, 2013.

Warren, S. G. and Wiscombe, W. J.: Dirty snow after nuclear war, Nature, 313, 467-470, 1985.

Wu, G., Wan, X., Gao, S., Fu, P., Yin, Y., Li, G., Zhang, G., Kang, S., Ram, K., and Cong, Z.: Humic-Like Substances (HULIS) in Aerosols of Central Tibetan Plateau (Nam Co, 4730 m asl): Abundance, Light Absorption Properties, and Sources, Environmental science & technology, 52, 7203-7211, 2018.

Wu, G., Xu, B., Zhang, C., Gao, S., and Yao, T.: Geochemistry of dust aerosol over the Eastern Pamirs, Geochimica Et Cosmochimica Acta, 73, 977-989, 2009.

Wu, G., Zhang, C., Li, Z., Zhang, X., and Gao, S.: Iron content and solubility in dust from high-alpine snow along a north-south transect of High Asia, 2012, 64, 2012.

Wu, G.-M., Cong, Z.-Y., Kang, S.-C., Kawamura, K., Fu, P.-Q., Zhang, Y.-L., Wan, X., Gao, S.-P., and Liu, B.: Brown carbon in the cryosphere: Current knowledge and perspective, Advances in Climate Change Research, 7, 82-89, 2016.

Yang, W., Guo, X., Yao, T., Zhu, M., and Wang, Y.: Recent accelerating mass loss of southeast Tibetan glaciers and the relationship with changes in macroscale atmospheric circulations, Climate Dynamics, doi: 10.1007/s00382-015-2872-y, 2015. 1-11, 2015.

Yasunari, T. J., Bonasoni, P., Laj, P., Fujita, K., Vuillermoz, E., Marinoni, A., Cristofanelli, P., Duchi, R., Tartari, G., and Lau, K. M.: Estimated impact of black carbon deposition during pre-monsoon season from Nepal Climate Observatory – Pyramid data and snow albedo changes over Himalayan glaciers, Atmos. Chem. Phys., 10, 6603-6615, 2010.

Zhang, X. L., Wu, G. J., Zhang, C. L., Xu, T. L., and Zhou, Q. Q.: What is the real role of iron oxides in the optical properties of dust aerosols?, Atmos. Chem. Phys., 15, 12159-12177, 2015.

Zhou, Y., Wang, X., Wu, X., Cong, Z., Wu, G., and Ji, M.: Quantifying Light Absorption of Iron Oxides and Carbonaceous Aerosol in Seasonal Snow across Northern China, Atmosphere, 8, 63, 2017.

Table 1 Summary of cryoconite samples collected from five glaciers over Tibetan Plateau and surroundings.

Glacier	Description	Coordinates	Elevation (m, a.s.l.)	Sampling date	Sample Number
Urumqi #1 Glacier (UG)	Tienshan Mount.	43º06´N, 86º48´E	3800-4000	Aug. 2014	14
LaoHuGou (LHG)	Qilian Mount.	39º28´N, 96º32´E	4300-4900	Jul. 2014	14
Xiaodongkemadi (XDK)	Tanggula Mount.	33º03´N, 92º04´E	5400-5600	Aug. 2014	6
PaLong #4 (PL)	Southeast TP	29°15'N, 96°56' E	4700	Sep. 2015	2
Baishui #1 Glacier (BS)	YuLong	27º6´N , 100º11´E	4600-4800	Aug. 2014	9

Table 2 The abundances (by mass) of total iron, free iron, hematite, goethite and their ratios determined in cryoconites from TP glaciers, as well as other data available in the literatures.

Locations	Description	Total iron (%)	Free iron (%)	Free-total iron ratio	Hematite %	Goethite %	Gt-Hm ratio	References
UG		4.62 (±0.22)[a]	1.41 (±0.29)	0.31 (±0.07)	0.24 (±0.02)	1.98 (±0.47)	8.26 (±2.27)	This study
LHG		4.28 (±0.17)	1.50 (±0.30)	0.35 (±0.07)	0.28 (±0.02)	2.08 (±0.48)	7.54 (±1.83)	This study
XDK	Cryoconite	3.40 (±0.18)	1.93 (±0.48)	0.56 (±0.12)	0.56 (±0.08)	2.44 (±0.69)	4.30 (± 0.90)	This study
PL		4.18(±0.13)	1.53(±0.28)	0.37(±0.08)	0.23(±0.01)	2.18(±0.44)	9.63(±1.88)	This study
BS		4.90 (±0.21)	3.43 (±0.53)	0.70 (±0.10)	0.10 (±0.01)	5.35 (±0.85)	55.2 (±10.4)	This study
Utah, USA	Dust on snow	1.73-2.85					~1[b]	Reynolds et al. (2014)
Niger, Sahara	Desert Aerosol	6.3 (±0.9)	2.8 (±0.8)	0.44 (±0.11)				Lafon et al. (2004)
Niger, Sahel	Desert Aerosol	7.8 (±0.4)	5.0 (±0.4)	0.65 (±0.04)				Lafon et al. (2004)
Yulin, China	Desert Aerosol	7.7 (±0.3)	3.7 (±0.4)	0.48 (±0.03)				Lafon et al. (2004)
ZBT, China	Desert aerosol	5.38 (±0.2)	3.0 (±0.2)	0.43 (±0.01)			~3.0	Lafon et al. (2006)
West Africa	Desert Aerosol			0.38-0.72	0.09-0.26[c]	0.21-0.49[c]	0.96-3.1	Formenti et al. (2014)

[a] Values in brackets represent the standard deviations; [b] Mössbauer spectroscopy indicated roughly equal amounts of hematite and goethite, while reflectance spectroscopy showed goethite was dominant iron oxides; [c] Using X-ray absorption (XAS). Note: the total and free iron data in this table were obtained from ICP-MS, so it refers to the elemental Fe. While hematite and goethite were measured as Fe oxides.

Fig. 1 Surface of mountain glacier (upper) in central Tibetan Plateau and dispersed cryoconite (down) on it.

5

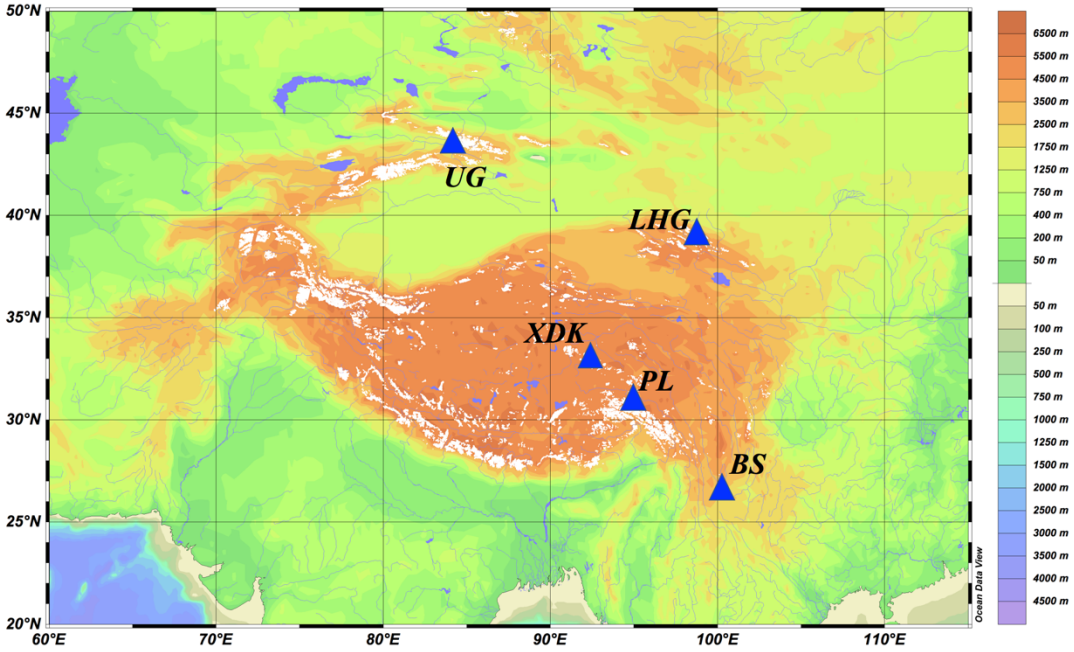

Fig. 2 Topographic map of the Tibetan Plateau and surrounding, with locations of five representative glaciers. Note: the base map was created by Ocean Data View software (Schlitzer, 2017).

5

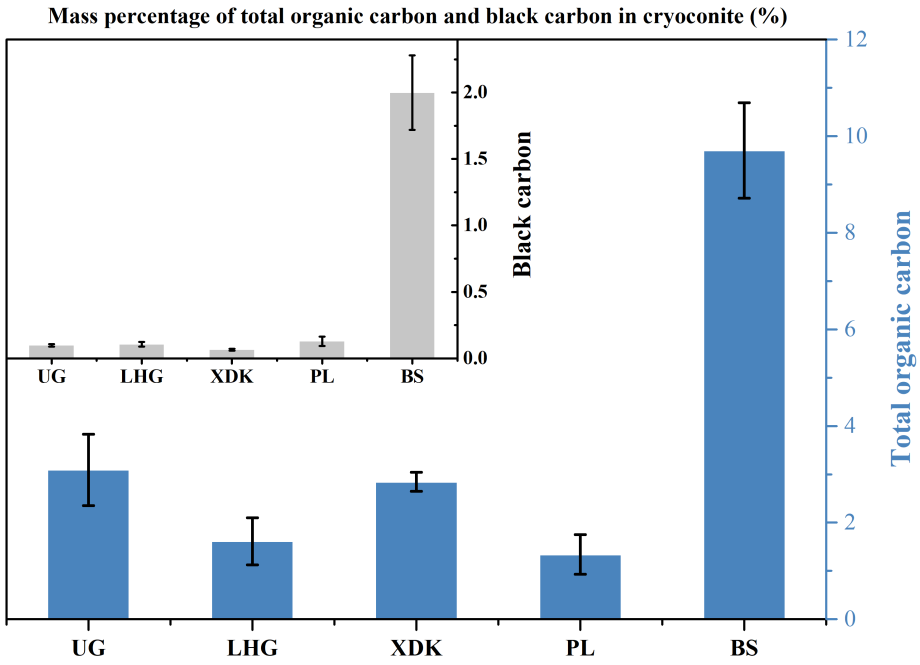

Fig. 3 The total organic carbon (blue) and black carbon (grey) in the total mass of cryoconites on the mountain glaciers of Tibetan Plateau and surroundings.

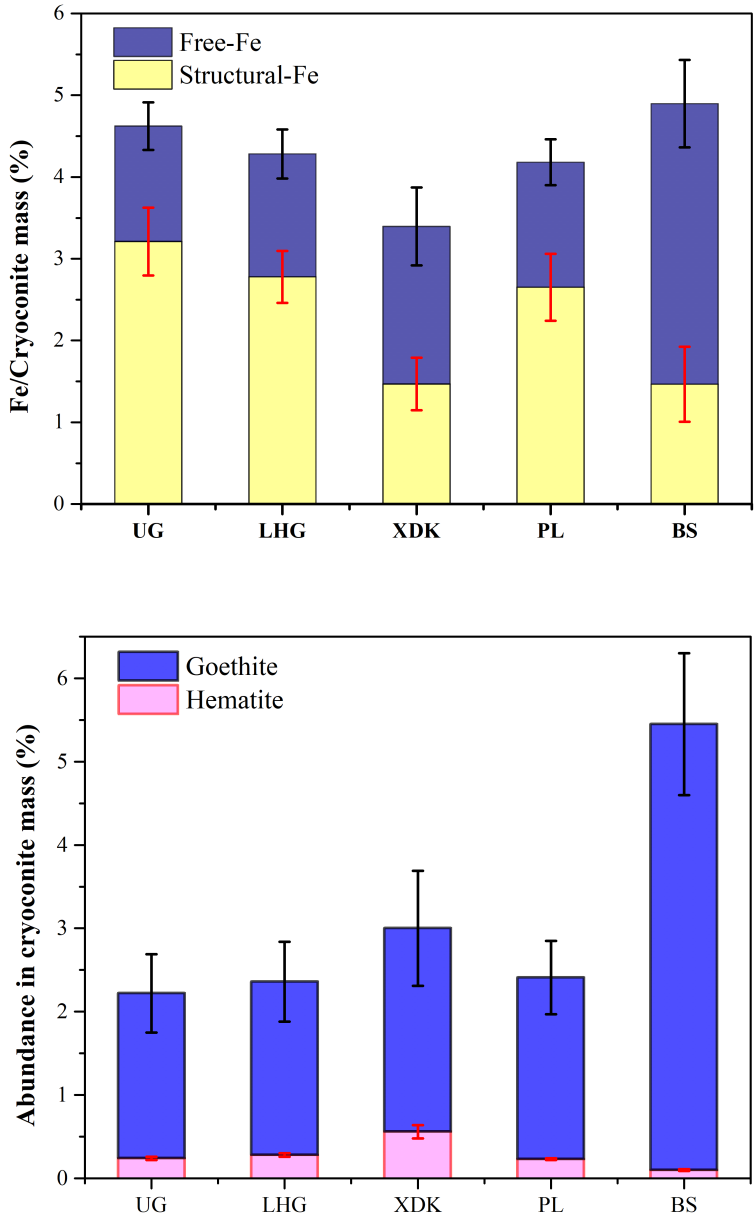

5

Fig. 4 The free iron and structural iron contents (elemental Fe) measured in the total cryoconite (dried) mass from TP glaciers (Upper), and goethite and hematite (Fe oxides) contents in the total cryoconite mass (Bottom).

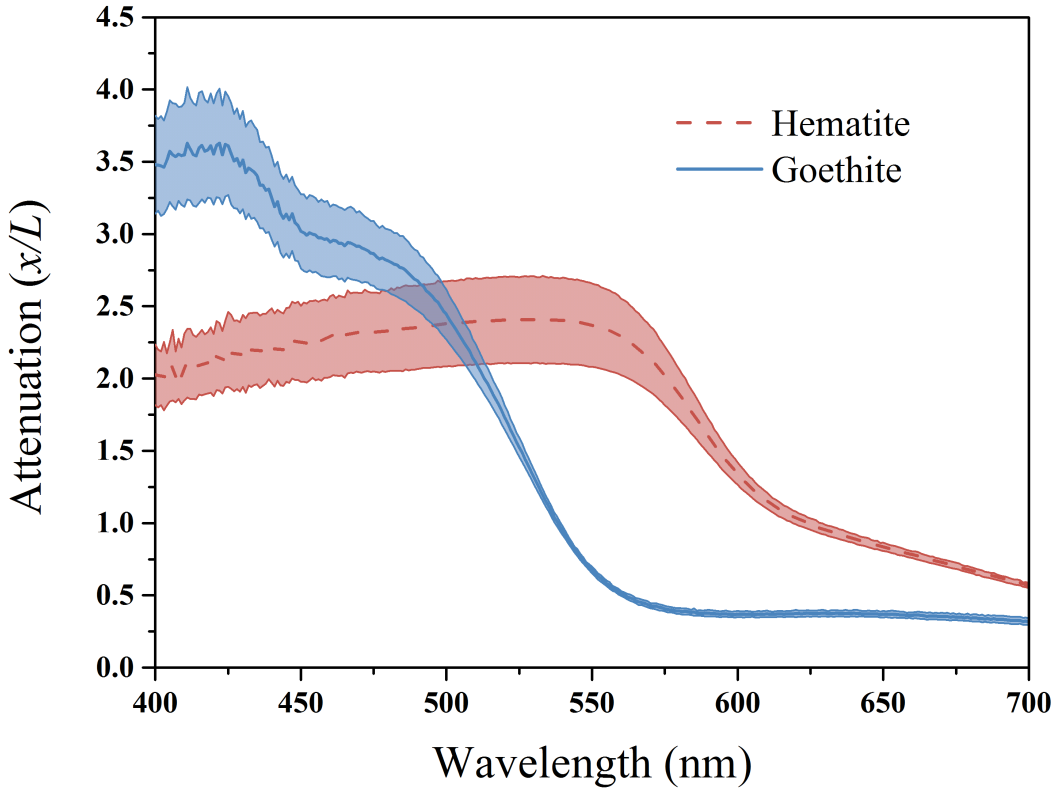

Fig. 5 The mass weighted light attenuation by hematite and goethite. Error bars indicate the standard deviation.

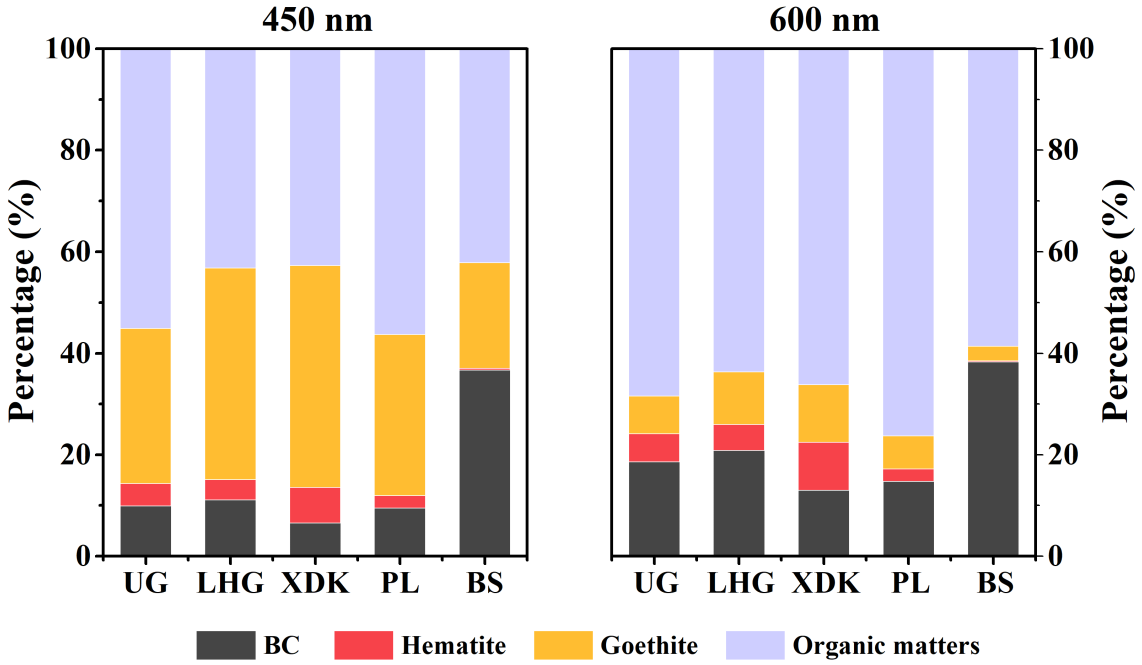

Fig. 6 Apportioning of total light absorption (450 nm and 600 nm, respectively) to black carbon, hematite, goethite and organic matters for the cryoconite from five TP glaciers.